Monte Carlo treatment of the transport of electrons in a gas including electron-electron interactions

A. Alkaa, P. Ségur, A. Zahraoui, and M. Kadri-H*
Centre de Physique Atomique, Unité de Recherche Associée au CNRS No. 277, 118 Route de Narbonne, 31062, Toulouse Cedex, France
(Received 11 March 1994)

A technique allowing electron-electron collisions to be included together with the electron–neutral-species (atom or molecule) collisions in a Monte Carlo simulation is developed for the case of a weakly ionized gas (ionization degree lower than 10^{-4}). The validity of this technique is checked by studying the evolution over time of a set of electrons (in an infinite medium) assuming that they collide only between each other. The space variation of the electron energy distribution function and some mean swarm parameters are calculated for a steady-state discharge established between two plane-parallel electrodes. The importance and the effect of the electron-electron collisions in argon are discussed and interpreted for two situations depending on the electron density at the cathode.

PACS number(s): 52.20.Fs, 52.80.−s, 51.50.+v, 52.65.+z

I. INTRODUCTION

It is well known that electron-electron collisions play an important role, together with electron–neutral-species collisions, in some gaseous discharges when the density of electrons increases sufficiently for the ionization degree to be higher than 10^{-5}. The change of the electron distribution function in this case may be very large compared to weakly ionized gases and a lot of work has been devoted to the theoretical determination of this electron distribution function taking into account electron-electron collisions [1–5].

Including electron-electron collisions in numerical modeling is made difficult by the nonlinear character of the interactions and, consequently, the more complex structure of the collision operator [4]. Usually, calculations are made using the Boltzmann equation approach and assuming a homogeneous, infinite medium. In this case, the Boltzmann equation is reduced to a nonlinear integro-differential equation with respect to the velocity variable whose solution can be obtained iteratively with standard numerical techniques [5–8]. All previous works based on the solution of the Boltzmann equation were concerned with equilibrium situations and the problem of nonequilibrium of electrons in space was never investigated. However, although it is known that one of the effects of electron-electron collisions is to push the distribution toward a Maxwellian and to make this distribution (at least in conservative cases) independent of position, the treatment of nonequilibrium situations in space when electron-electron interactions can no longer be ignored is also important, but no method is, for the moment, applicable to this situation.

The Boltzmann equation approach is very difficult to implement in this case, and it seems necessary to develop a method that is more flexible to include electron-electron interactions in nonequilibrium situations. The simplest method of studying the transport of electrons through gases is the Monte Carlo (MC) method. It has been widely used in the literature [9–11] but only electron–neutral-species collisions were taken into account and the electron-electron interactions were always ignored except in a few Monte Carlo calculations [7].

The aim of the present part is, first, to show how it is in fact possible to include, in a very simple way, electron-electron interactions (long-range interaction, cross sections dependent on the relative velocity) in Monte Carlo calculations, and, second, to apply this formulation to the study of the transport of electrons in a stationary discharge where electrons are not necessarily in equilibrium with the electric field.

In the first part of this paper, we will give a brief but comprehensive review of the Monte Carlo method applied to the simulation of electron trajectories in a background gas acted on by a uniform electric field. In the second part, we will show how to extend the Monte Carlo method to the treatment of electron-electron collisions. The validity of this treatment will be first checked in simple situations (see Sec. III) and some numerical results will be given and discussed for more realistic cases.

II. BRIEF DESCRIPTION OF THE TRADITIONAL MONTE CARLO METHOD

As many Monte Carlo studies have already been reported in the literature, we will not detail the whole procedure used in this work. The interested reader can refer to standard textbooks or papers published on the subject [7,9,10,12,13]. Only the most characteristic features of our procedure will be given in the following.

One of the most striking steps in a Monte Carlo calculation is the determination of the physical parameters that characterize a collision (time, position, energy, angle, etc.) If an electron is emitted somewhere in the gas at time t_0, it may undergo a collision at time t_1. The free flight time $\Delta t = t_1 - t_0$ between two collisions is calculated using the usual relationship:

*Present address: Laboratoire d'Electronique et Traitement du Signal, Avenue Ibn Battouta, B.P. 1014 Rabat, Maroc.

$$\ln\left[\frac{1}{1-R_{\Delta t}}\right]=\int_{t_0}^{t_1}\nu_{\text{tot}}(\varepsilon(t))dt \ , \tag{1}$$

in which $R_{\Delta t}$ is a pseudorandom number, uniformly weighted on the interval [0,1]. The quantity $\nu_{\text{tot}}(\varepsilon(t))$ is the total frequency of the electron–neutral-species collisions and $\varepsilon(t)$ is the kinetic energy of the electron at time t.

To determine t_1, i.e., the time at which the next collision occurs, it is necessary to invert Eq. (1) above. As ν_{tot} is usually a function of the electron energy, (1) is difficult to solve. To facilitate the solution, the "null collision" technique introduced for the fist time by Skullerud in 1968 [14] (see also [15,16]) is used in this work as in most modern Monte Carlo treatments of the motion of electrons in ionized gases. The "null collision" ν_{nul} is a fictitious collision which does not affect the electron velocity, and whose frequency is chosen so that the total collision frequency ν_{max} (including the null collision) is constant. We have

$$\nu_{\text{max}}=\nu_{\text{nul}}(\varepsilon(t))+\nu_{\text{tot}}(\varepsilon(t)) \ .$$

ν_{max} is then greater than or equal to the maximum of $\nu_{\text{tot}}(\varepsilon(t))$.

Once ν_{max} is substituted instead of $\nu_{\text{tot}}(\varepsilon(t))$ in Eq. (1), the quadrature is easily made and we obtain the following relationship:

$$\Delta t=t_1-t_0=\frac{-\ln R_{\Delta t}}{\nu_{\text{max}}} \ ,$$

which gives the time of the next collision whatever its type (real or fictitious).

Once the collision time is obtained, the velocity, energy, and position of the electrons are determined using standard classical kinematic relations. The nature of this collision is then chosen stochastically. The direction of the velocity of the electron after the collision is again determined stochastically according to the differential angular cross sections for the type of collision considered.

The procedure described above is very common in most current Monte Carlo codes. What is very often different in Monte Carlo techniques is the calculation of the various macroscopic or microscopic parameters [11].

In our procedure, the space and time variations of the various quantities are calculated considering the state of the electron before every collision (real or null). For every interval in the phase space considered, all the data indexed by "l" (time t_l, position z_l, kinetic energy ε_l, velocity v_{zl}, angle between velocity and electric field θ_l) are recorded just before a collision named "l." In these conditions, if x_l is a variable characteristic of the electron motion just before a collision, the Dirac function δ used below is equal to 1 if x_l belongs to the interval $[x_i,x_{i+1}]$ and zero otherwise.

The density $n(t_i,z_j)$ at time t_i and position z_j, proportional to the real electron density $n_e(t,z)$, is then given by the relationship

$$n(t_i,z_j)=\sum_{l=1}^{N_{\text{col}}}\delta(t_l-t_i)\delta(z_l-z_j) \ .$$

N_{col} is the total number of collisions made by the electrons during the whole simulation.

In the same way, we can introduce the mean energy

$$\langle\varepsilon\rangle(t_i,z_j)=\frac{1}{n(t_i,z_j)}\sum_{l=1}^{N_{\text{col}}}\delta(t_l-t_i)\delta(z_l-z_j)\varepsilon_l \ ,$$

the component of the mean velocity along the direction of the electric field

$$\langle v_z\rangle(t_i,z_j)=\frac{1}{n(t_i,z_j)}\sum_{l=1}^{N_{\text{col}}}\delta(t_l-t_i)\delta(z_l-z_j)v_{zl} \ ,$$

and the excitation or ionization frequency

$$\Omega_k(t_i,z_j)=\frac{1}{n(t_i,z_j)}\sum_{l=1}^{N_{\text{col}}}\delta_{k,l}\delta(t_l-t_i)\delta(z_l-z_j)\nu_{\text{max}} \ ,$$

where k designates the type of collision (excitation or ionization). Note that $\delta_{k,l}$ is equal to 1 if collision "l" occurring at time t_l is an excitation or an ionization and is otherwise equal to 0.

Using ionization frequency and mean velocity, we can also introduce the ionization coefficient which characterizes the ionizing power of electrons along unit length, and we have

$$\alpha_{\text{ion}}(t_i,z_j)=\frac{\Omega_k(t_i,z_j)}{\langle v_z\rangle(t_i,z_j)} \ .$$

We can also define the energy distribution function $f(t_i,z_j,\varepsilon_k)$ by the following relationship:

$$f(t_i,z_j,\varepsilon_k)=\frac{1}{n(t_i,z_j)}\sum_{l=1}^{N_{\text{col}}}\delta(t_l-t_i)\delta(z_l-z_j)\delta(\varepsilon_l-\varepsilon_k)$$

and the corresponding angular energy distribution function

$$f(t_i,z_j,\varepsilon_k,\theta_m)=\frac{1}{n(t_i,z_j)}\sum_{l=1}^{N_{\text{col}}}\delta(t_l-t_i)\delta(z_l-z_j)\delta(\varepsilon_l-\varepsilon_k)$$
$$\times\delta(\theta_l-\theta_m)\sin(\theta_l) \ ,$$

where θ is the angle between the electron velocity and the Oz axis (orthogonal in our case with the electrodes).

We must note that, in our procedure, the accuracy of the MC method increases with the number of collisions because all the information about the motion of electrons is stored before each collision (real or null). Consequently, as we cannot modify the number of real collisions (since the corresponding cross sections are fixed), it is possible to increase the accuracy of our results by changing the null collision frequency as the null collisions do not affect the motion of electrons (Fig. 1).

The only procedure to increase the number of null collisions is to increase ν_{max}. In the present work, this frequency is increased until stable results are obtained.

The above description is a rapid review of the Monte Carlo calculation of swarm parameters and distribution

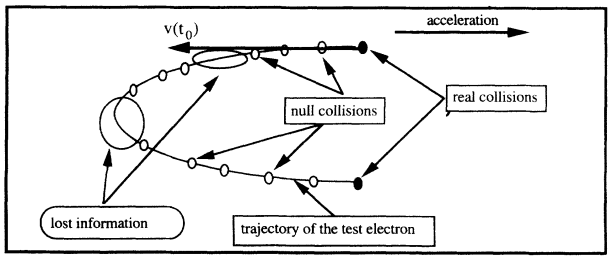

FIG. 1. Example of null collision distribution between two real collisions along the trajectory of the test electron.

functions of electrons in a weakly ionized gas taking into account only the electron–neutral-species collisions. In Sec. III we will add the electron-electron interactions to the above treatment. We must note that, in doing so, we will go from a linear Monte Carlo procedure in which the frequency $\nu_{\max}$ is determined only from the knowledge of the electron–neutral-species cross sections and independent of the density of electrons inside the gas to a nonlinear one in which $\nu_{\max}$ depends on the electron distribution function.

III. TECHNIQUE OF SIMULATION OF ELECTRON-ELECTRON COLLISIONS

In the following, we will distinguish two parts according to how we treat the interaction, approximately or accurately. In the first part, we will describe an approximate treatment of the electron-electron collisions as was done in [7]. In the second part, the electron-electron interaction will be taken into account accurately, the Rutherford formula being used to determine the electron-electron differential collision cross section.

A. Approximate treatment of electron-electron collisions

Unlike the case of electron–neutral-species collisions, the interaction strength between two electrons is a long-range interaction which produces a small-angle deflection. That means that, in a sufficiently ionized gas, the test electron experiences weak interactions with many electrons simultaneously. We are then faced with a multibody encounter theory problem. To simplify the treatment in this case, we can consider the multi-interaction as a fictitious local binary collision. In these conditions, the electron-electron interaction frequency is given by the following equation (see [7]):

$$\nu_{e\text{-}e}(\mathbf{v})=\frac{n_e}{N}N\int v_r\sigma_{e\text{-}e}(v_r)F(\mathbf{r},\mathbf{v}_t,t)d^3v_t \ , \tag{2}$$

with $v_r=|\mathbf{v}-\mathbf{v}_t|$, where $\mathbf{v}$ is the velocity of the test electron, $\mathbf{v}_t$ is the velocity of the target electron, $\sigma_{e\text{-}e}$ is the microscopic electron-electron cross section, and $F(\mathbf{r},\mathbf{v}_t,t)$ is the distribution function of electrons at time t and position $\mathbf{r}$. N is the density of the neutral background gas. Obviously, v_r is the modulus of the relative velocity between the two electrons. In these conditions, it is clear that, as $\nu_{e\text{-}e}(\mathbf{v})$ depends on the distribution F, it can only be determined if F is known. As F will only be known if $\nu_{e\text{-}e}(\mathbf{v})$ is known, it follows that the determination of the distribution F will be necessarily made in an iterative manner.

To describe the conservative binary interaction between two identical particles, it is necessary first to know the velocity of particles before the collision. Once the velocity of these particles is known, the velocity of particles after the collision is determined using the laws of conservation of energy and momentum together with the angular differential cross section. In the case of electron-electron collisions only the velocity $\mathbf{v}$ of the test electron before the collision is known. The velocity $\mathbf{v}_t$ of the target electron is sampled in agreement with the distribution F using a pseudorandom number uniformly weighted on the interval [0,1]. Using this method, expression (2) becomes

$$\nu_{e\text{-}e}(\mathbf{v})=\frac{n_e}{N}Nv_r\sigma_{e\text{-}e}(v_r) \ .$$

The calculations start with an approximate distribution F (for example, obtained ignoring electron-electron collisions) and continue in the same way with F updated after every collision. Obviously, after a large number of electron-electron collisions the real distribution function $F(\mathbf{r},\mathbf{v}_t,t)$ will be obtained. For simplification, the direction of the target electron velocity was determined considering that the angular distribution was isotropic [7].

The cross section of the electron-electron collision was given by the approximate relationship [7]

$$\sigma_{e\text{-}e}(v_r)=\frac{e^4\ln(\Lambda)}{4\pi\varepsilon_0^2(mv_r^2)^2} \ , \tag{3}$$

with

$$\Lambda=\frac{12\pi(\varepsilon_0 kT_e/e^2)^{3/2}}{n_e^{1/2}} \ ,$$

where e and m are, respectively, the charge and the mass of an electron; T_e is the electron temperature; k is Boltzmann's constant; and ε_0 is the permittivity of free space.

The constant total frequency $\nu_{\max}$ used to calculate the time of flight was determined in the following way: Expression (3) above shows that the electron-electron collision frequency becomes infinite when v_r vanishes. Therefore, the constant frequency $\nu_{\max}$, needed to calculate the time of flight, also reaches infinity. This problem was solved by choosing a lower limit $v_{r\min}$ to v_r and then adding $n_e v_{r\min}\sigma_{e\text{-}e}(v_{r\min})$ to the maximum of ν_{tot} previously calculated taking into account only the electron–neutral-species collisions. Obviously, the results of the calculation depend on the value chosen for $v_{r\min}$. However, it is easy to verify that when v_r approaches zero, the energy exchange during an electron-electron collision becomes negligible even if the scattering angle is large. So when v_r vanishes, the effect of the electron-electron collisions is less important, even if the cross section becomes infinite. In these conditions the results of the calculations are not strongly dependent on $\nu_{r\min}$ if a sufficiently low value of this limit is chosen.

B. Accurate treatment of electron-electron collisions

The Rutherford scattering $\sigma_{e\text{-}e}(v_r,\chi)$ formula giving the differential cross section is

$$\sigma_{e\text{-}e}(v_r,\chi)=\frac{b_0^2}{(1-\cos\chi)^2}\ , \tag{4}$$

where

$$b_0=\frac{e^2}{4\pi\varepsilon_0\mu v_r^2} \tag{5}$$

and μ is the reduced mass equal to $m/2$.

When the scattering angle χ reaches zero, the differential cross section becomes infinite, but at the same time the energy exchange and the momentum transfer can be ignored. It follows that the effect of electron-electron collisions is less important when the scattering angle is low. For this reason it seems better to take into account the electron-electron collisions using the momentum transfer cross section $\sigma_{mee}(v_r)$ defined by

$$\begin{aligned}\sigma_{mee}(v_r)&=2\pi\int_{\chi_{\min}}^{\pi}\sigma_{e\text{-}e}(v_r,\chi)(1-\cos\chi)\sin\chi\,d\chi\\&=2\pi b_0^2\int_{\chi_{\min}}^{\pi}\frac{\sin\chi}{(1-\cos\chi)}d\chi\\&=2\pi b_0^2\ln\frac{2}{1-\cos\chi_{\min}}\ ,\end{aligned} \tag{6}$$

where $\chi_{\min}$ is the lower limit of the scattering angle obtained by considering the *screening effect of the Coulomb potential* (for more information, the reader is referred to [4]).

$\chi_{\min}$ depends on the Debye length λ_D and also on the relative velocity v_r between the two interacting electrons. Using another formula of the momentum transfer cross section [4], it is possible to determine $\chi_{\min}$:

$$\sigma_{mee}(g)=2\pi b_0^2\ln\left[1+\frac{\lambda_D^2}{b_0^2}\right]\ ; \tag{7}$$

then

$$\cos\chi_{\min}=\frac{\lambda_D^2-b_0^2}{\lambda_D^2+b_0^2}\ , \tag{8}$$

with

$$\lambda_D=\left[\frac{\varepsilon_0 KT_e}{e^2 n_e}\right]^{1/2}\ .$$

Note that KT_e equals $\frac{2}{3}\langle\varepsilon\rangle(t,z)$, assuming that t and z are the time and position of the current collision.

When the relative velocity v_r reaches zero according to expressions (6) and (8), $\chi_{\min}$ goes to π. This means that the scattering angle is greater when the relative velocity is low.

Note that, now, there is no approximation on $\sigma_{mee}(v_r)$ compared to the cross section $\sigma_{e\text{-}e}(v_r)$ used in [7]. Note also that the constant total frequency $\nu_{\max}$ including the electron-electron collision frequency $\nu_{e\text{-}e}(\mathbf{v})$ [equal here to $n_e v_r \sigma_{mee}(v_r)$] is calculated in the same way as in Sec. III A.

During the simulation, it is possible that the sum $n_e v_r \sigma_{mee}(v_r)+\nu_{\text{tot}}$ becomes higher than $\nu_{\max}$. If this situation occurs, the simulation is stopped and a new value of $\nu_{\max}$ is calculated. Once $\nu_{\max}$ is determined correctly, the main difficulty is to calculate the relative velocity v_r between the test electron and the target electron with velocities $\mathbf{v}(t_1)$ and $\mathbf{v}_t(t_1)$, respectively, at time t_1.

The energy and the components of the velocity $\mathbf{v}(t_1)$ of the test electron in the O_x, O_y, and O_z directions just before the collision occurring at time t_1 are known, and are given by the following relationships

$$\begin{aligned}&v_x(t_1)=v_x(t_0)\ ,\\&v_y(t_1)=v_y(t_0)\ ,\\&v_z(t_1)=\frac{eE}{m}\Delta t+v_z(t_0)\ ,\\&\varepsilon(t_1)=\varepsilon(t_0)+\tfrac{1}{2}m[v_z^2(t_1)-v_z^2(t_0)]\ .\end{aligned}$$

The components v_{tx}, v_{ty}, and v_{tz} of the velocity $\mathbf{v}_t(t_1)$ are determined as described above according to the energy and angular distributions of electrons in the medium and using three pseudorandom numbers R_ε, $R_{\theta t}$, and $R_{\psi t}$:

$$\begin{aligned}&v_{tx}=v_t\sin\theta_t\cos\psi_t\ ,\\&v_{ty}=v_t\sin\theta_t\sin\psi_t\ ,\\&v_{tz}=v_t\cos\theta_t\ ,\end{aligned}$$

with

$$v_t=\left[\frac{2\varepsilon_t}{m}\right]^{1/2}\ .$$

The energy of the target electron ε_t is determined using the energy distribution function $f(t_1,z(t_1),\varepsilon)$ of all electrons previously followed, according to the expression

$$R_\varepsilon=\frac{\int_0^{\varepsilon_t}f(t_1,z(t_1),\varepsilon)d\varepsilon}{\int_0^{\varepsilon_{\max}}f(t_1,z(t_1),\varepsilon)d\varepsilon}\ .$$

Then the angle θ_t is determined using the angular distribution $f(t_1,z(t_1),\varepsilon_t,\theta)$ of electrons already treated:

$$R_{\theta t}=\frac{\int_0^{\theta_t}f(t_1,z(t_1),\varepsilon_t,\theta)d\theta}{\int_0^{\pi}f(t_1,z(t_1),\varepsilon_t,\theta)d\theta}\ .$$

In most cases the computer memory is not sufficient to store $f(t,z,\varepsilon,\theta)$. However, as in the present paper, for which the calculations were made in two situations where the system was only space or time dependent, respectively, it follows that knowledge of the full distribution $f(t,z,\varepsilon,\theta)$ is not necessary and that only the distribution functions $f(t,\varepsilon,\theta)$ or $f(z,\varepsilon,\theta)$ are needed to sample θ_t.

For the same reason [insufficient computer memory to store $f(t,\varepsilon,\theta,\psi)$ or $f(z,\varepsilon,\theta,\psi)$], the azimuthal angle ψ_t was determined according to an isotropic distribution,

$$\psi_t=2\pi R_{\psi_t}\ .$$

Finally, from these calculations, the relative velocity v_r between the test electron and the target electron is given by

$$v_r=(v_{r_x}^2+v_{r_y}^2+v_{r_z}^2)^{1/2},$$

with

$$v_{rx}=v_x(t_1)-v_{tx}=v_r\sin\theta_r\cos\varphi_r ,$$
$$v_{ry}=v_y(t_1)-v_{ty}=v_r\sin\theta_r\sin\varphi_r ,$$
$$v_{rz}=v_z(t_1)-v_{tz}=v_r\cos\theta_r .$$

The values of the angles θ_r and φ_r are easily calculated from the values of v_{rx}, v_{ry}, and v_{rz}.

This value of v_r is used to calculate the probability at t_1 of the electron-electron collision given by the relationship

$$P_{e\text{-}e}(\mathbf{v})=\frac{\nu_{e\text{-}e}(\mathbf{v})}{\nu_{\max}}$$

(see above). This probability is used in the determination of the nature of the collision occurring at time t_1 in the same way as in Sec. II.

If the collision is an electron-electron collision, the components $v_{r'x}$, $v_{r'y}$, and $v_{r'z}$ of the relative velocity after the collision in the reference (O_x,O_y,O_z) are given by

$$\begin{aligned}v_{r'x}=v_{r'}\{&-\sin\chi\sin\psi\sin\varphi_r\\&+\sin\chi\cos\psi\cos\theta_r\cos\varphi_r\\&+\cos\chi\sin\theta_r\cos\varphi_r\},\end{aligned}$$
$$\begin{aligned}v_{r'y}=v_{r'}\{&+\sin\chi\sin\psi\cos\varphi_r\\&+\sin\chi\cos\psi\cos\theta_r\sin\varphi_r\\&+\cos\chi\sin\theta_r\sin\varphi_r\},\end{aligned}$$
$$v_{r'z}=v_{r'}\{-\sin\chi\cos\psi\sin\theta_r+\cos\chi\cos\theta_r\} .$$

In the relationships above, $v_{r'}=v_r$ (since the collision is elastic), χ is the scattering angle, and ψ is the angle of the relative orientation of the collision plane.

The momentum transfer cross section having been used to take into account the electron-electron interaction, the angle χ is determined using a pseudorandom number $R_{\chi ee}$ according to the following relationships:

$$R_{\chi ee}=\frac{\int_{\chi\min}^{\chi}\sigma_{e\text{-}e}(v_r,\chi')(1-\cos\chi')\sin\chi'd\chi'}{\int_{\chi\min}^{\pi}\sigma_{e\text{-}e}(v_r,\chi')(1-\cos\chi')\sin\chi'd\chi'} ,$$

$$\cos\chi=1-(1-\cos\chi_{\min})\exp\left[R_{\chi ee}\ln\frac{2}{1-\cos\chi_{\min}}\right] .$$

Since the Coulomb potential is isotropic, the angle ψ is determined in the same way as for the electron–neutral-species collisions using a pseudorandom number $R_{\psi ee}$:

$$\psi=2\pi R_{\psi ee} .$$

The velocity components and the energy of the test electron after the electron-electron collision are calculated by [7]

$$v_x'(t_1)=\tfrac{1}{2}[v_x(t_1)+v_{tx}+v_{r'x}] ,$$
$$v_y'(t_1)=\tfrac{1}{2}[v_y(t_1)+v_{ty}+v_{r'y}] ,$$
$$v_z'(t_1)=\tfrac{1}{2}[v_z(t_1)+v_{tz}+v_{r'z}] ,$$
$$\varepsilon'(t_1)=\tfrac{1}{2}m[v_{r'x}^2(t_1)+v_{r'y}^2(t_1)+v_{r'z}^2(t_1)] .$$

Finally, the simulation of the motion of the test electron through the background gas is continued until the disappearance of the electron. Then a large number of electrons are followed until good statistics are obtained.

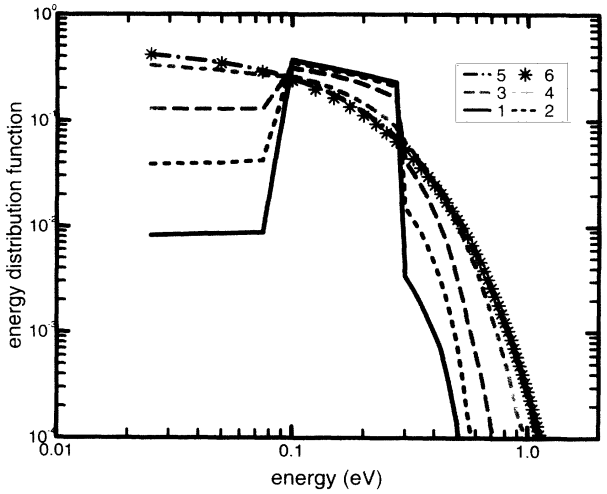

FIG. 2. Energy distribution function taking into account only the electron-electron interactions for different times. The electron density equals $7.08\times10^{+17}$ cm^{-3}. (1) $t=1.25$ ps, (2) $t=6.25$ ps, (3) $t=23.75$ ps, (4) $t=98.75$ ps, (5) $t=246.25$ ps, and (6) Maxwellian distribution at a mean energy of 0.2 eV.

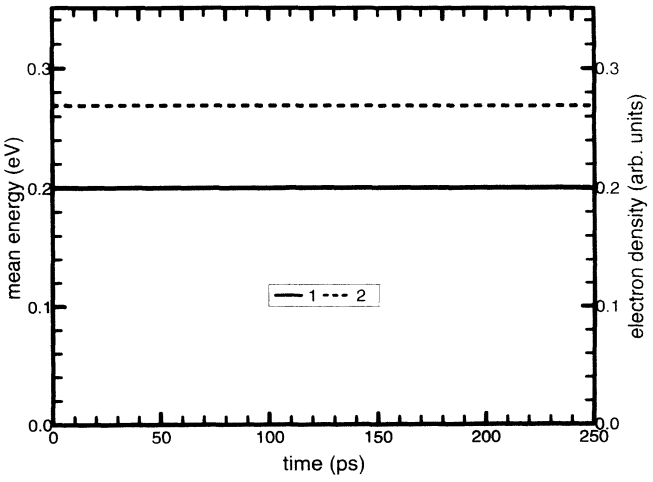

FIG. 3. Time variation of the mean energy (1) and of the electron density (2). The conditions are the same as in Fig. 2.

IV. NUMERICAL RESULTS

A. Check of the accuracy of the method

A very simple way to check the validity of our method is to follow the evolution over time of a set of electrons moving in an infinite medium and undergoing only electron-electron interactions. If we assume that the medium is homogeneous, i.e., the distribution function does not depend on space, it can easily be shown from the first hydrodynamic equations that the density and the mean energy of electrons are independent of time. Furthermore, whatever the initial energy distribution of the electrons, the final equilibrium distribution function will be Maxwellian [5].

In Fig. 2 we plot the energy distribution function for different times. The initial distribution function is rectangular between 0.1 and 0.3 eV, so the initial mean energy equals 0.2 eV. Figure 2 shows clearly that, starting from this initial situation, the distribution function be-

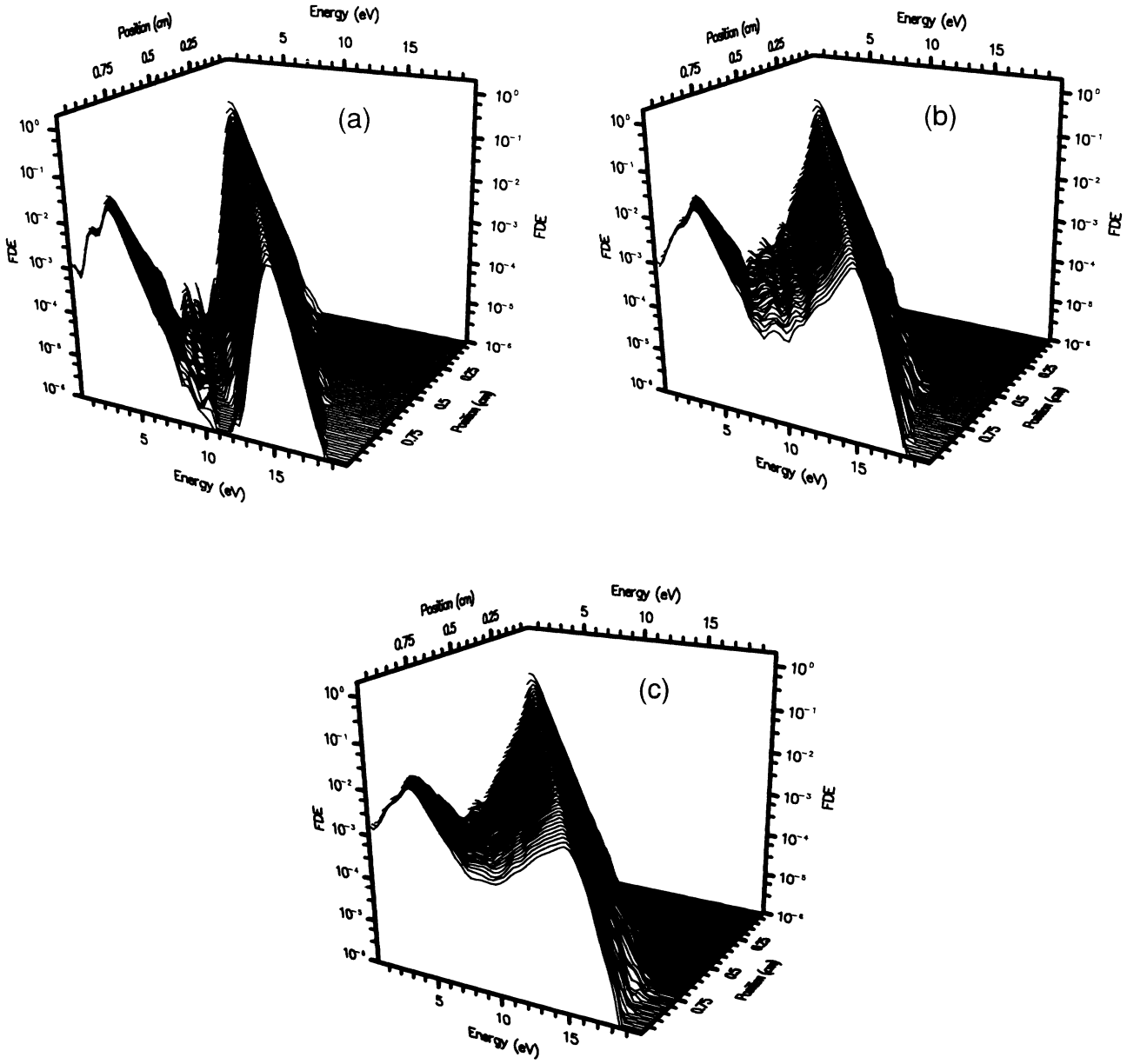

FIG. 4. (a) Energy and space variation of the distribution function in argon without electron-electron interactions for $E/N=42.373$ Td and $Nd=3.54\times10^{+16}$ cm^{-2}. (b) Energy and space variation of the distribution function in argon taking into account the electron-electron interactions for $E/N=42.373$ Td and $Nd=3.54\times10^{+16}$ cm^{-2} $n_{e0}/N=10^{-5}$. (c) Energy and space variation of the distribution function in argon taking into account the electron-electron interactions for $E/N=42.373$ Td and $Nd=3.54\times10^{+16}$ cm^{-2} $n_{e0}/N=3\times10^{-5}$.

comes Maxwellian. Figure 3 shows the time variation of mean energy and electron density. Clearly, as postulated, these two quantities do not depend on time. These results confirm that the hypotheses and the techniques used in the present paper to include the electron-electron interactions are valid and lead to accurate treatment using the Monte Carlo method.

B. Results in the case of a steady-state discharge

It is well known that one of the effects of electron-electron interactions is to make the distribution function closer and closer to Maxwellian. This is the traditional situation observed in the positive column of a glow discharge. In this case, the electron and ion densities are very high, the mean energy of electrons is low, and electron-electron interactions are numerous. It is possible that electron-electron interactions play a very important role in some other regions of a glow discharge—for example, during the transition from the cathode fall to the negative glow. In this case, the number of electrons created in the cathode fall and that penetrate inside the negative glow is high and electron-electron interactions are likely to be important. To estimate the importance of this effect, it is necessary to be able to study the transport of electrons in a nonhomogeneous discharge, taking into account electron-electron collisions. In the following, we limit our investigation to a simple situation where the electric field in the discharge is constant and we will study the role played by most physical quantities on the importance of electron-electron interactions.

In this case, electrons move between plane-parallel electrodes through an argon background gas and are subjected to a constant electric field. The physical situation

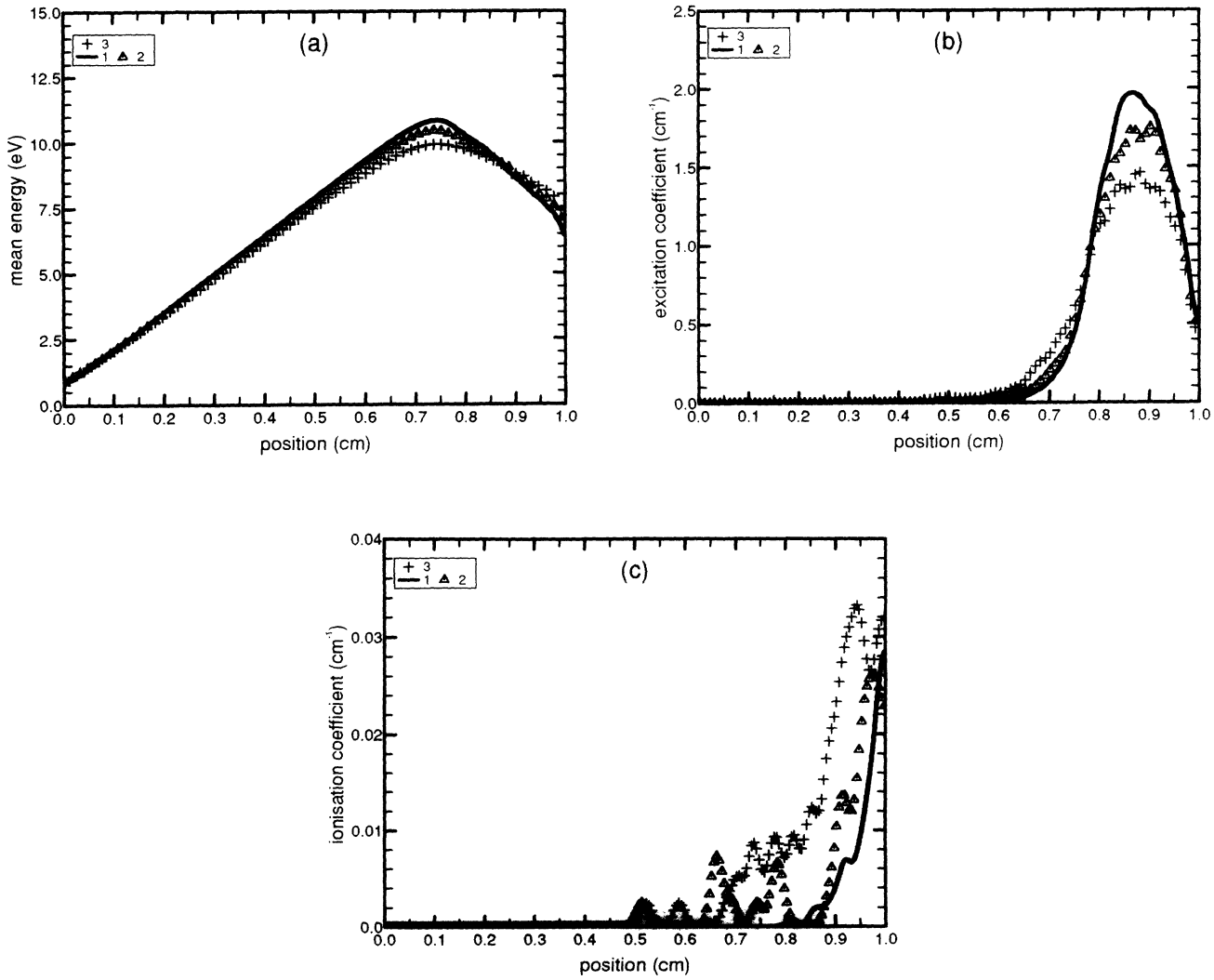

FIG. 5. (a) Space variation of mean energy in argon (1) without electron-electron interactions and with for (2) $n_{e0}/N=10^{-5}$ and (3) $n_{e0}/N=3\times10^{-5}$. The conditions are the same as in Fig 3. (b) Space variation of excitation coefficient as in (a). (c) Space variation of ionization coefficient as in (a).

is then characterized by the ratio E/N (the ratio of the electric field E to the density N of the background gas); the product Nd, where d is the gap distance; the mean energy ε_{c0} of electrons; and the ionization degree n_{e0}/N at the cathode. The set of electron-atom collision cross sections of argon used in this paper is taken from [17].

In Figs. 4, 6, and 8, we plot the space variation of the energy distribution of electrons for three different E/N values: 42.373, 56.497, and 141.243 Td, respectively. Parts (a) of the figures correspond to situations where electron-electron interactions are ignored. (b) and (c) correspond to situations where electron-electron interactions are taken into account with an ionization degree at the cathode of 10^{-5} and 3.10^{-5}, respectively.

Figure 5 gives (a) the space variation of mean energy, (b) the excitation coefficient of some forbidden transitions and (c) the ionization coefficient, without and with electron-electron interactions for E/N equal to 42.373

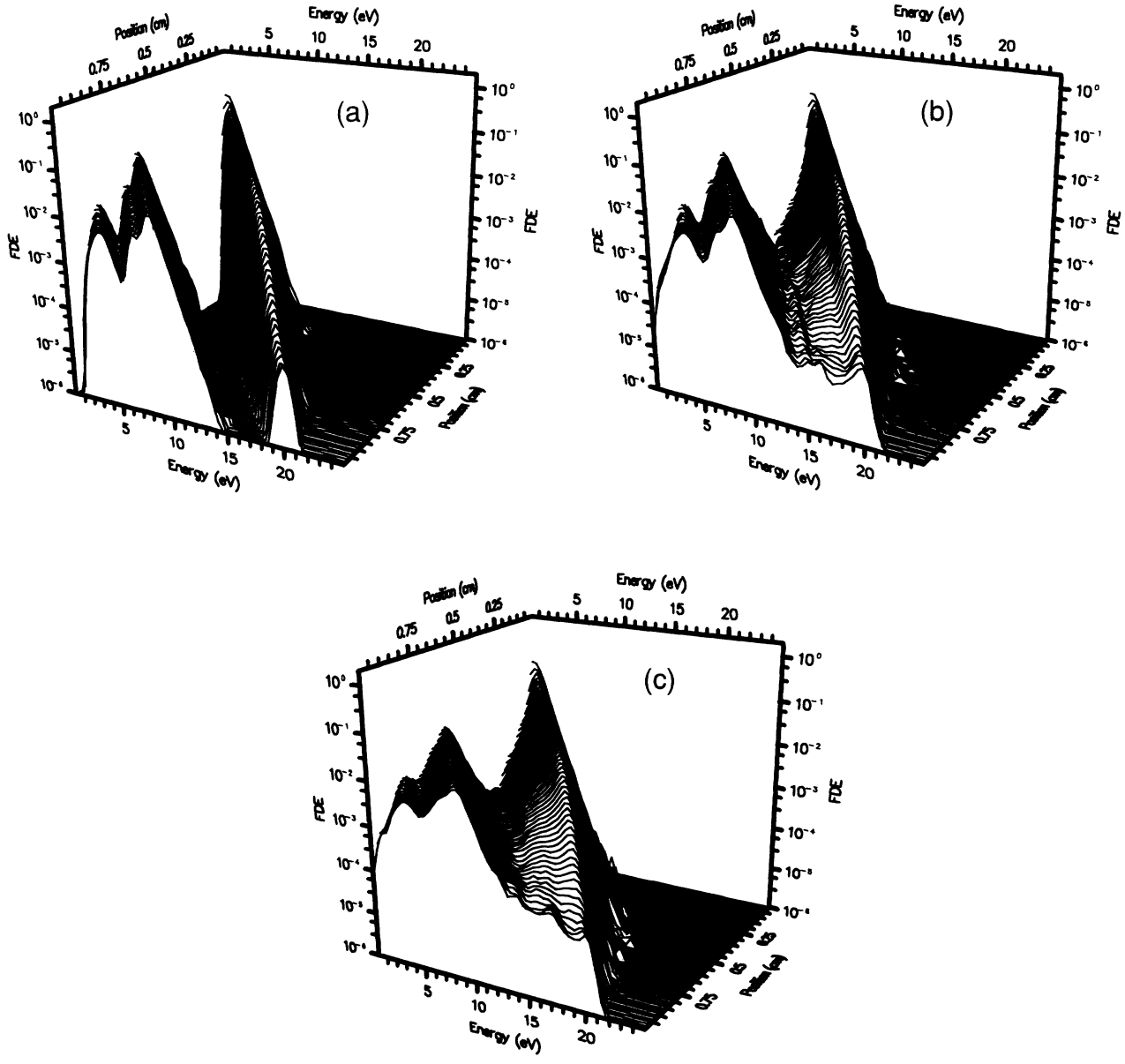

FIG. 6. (a) Energy and space variation of the distribution function in argon without electron-electron interactions for $E/N=56.497$ Td and $Nd=3.54\times10^{+16}$ cm^{-2}. (b) Energy and space variation of the distribution function in argon taking into account the electron-electron interactions for $E/N=56.497$ Td and $Nd=3.54\times10^{+16}$ cm^{-2} $n_{e0}/N=10^{-5}$. (c) Energy and space variation of the distribution function in argon taking into account the electron-electron interactions for $E/N=56.497$ Td and $Nd=3.54\times10^{+16}$ cm^{-2} $n_{e0}/N=3\times10^{-5}$.

Td. Figures 7 and 9 give the same swarm parameters in the same conditions except that E/N is equal to 56.497 and 141.243 Td, respectively.

Figures 4(a), 6(a), and 8(a) show the energy and space variation of the distribution function without electron-electron interactions for three different E/N values. In every case, the electrons leaving the cathode are accelerated by the electric field and move inside a band, the width of which is characterized by the width of the initial energy of electrons released at the cathode. When the energy of the electrons is sufficiently high, they experience inelastic collisions and they lose energy. This energy loss is less when E/N [Fig. 4(a)] is small than when E/N is high [Fig. 8(a)]. As they lose energy, electrons create some new bands whose width is identical to the first one. At low E/N, only one band is created but as E/N grows, more bands appear. Due to the existence of different excitation and ionization processes, several bands appear at high E/N [Fig. 8(a)] which overlap as electrons move far from the cathode.

When electron-electron interactions are not taken into account, the width of the various bands is well defined (being controlled only by the values of the excitation and the ionization threshold of the atoms) and some empty regions appear between the bands.

With electron-electron interactions, the situation is different; the electrons are able to move in a continuous way along the energy axis, the distribution function spreading through energy space, and there are no empty regions between bands. The number of electrons filling these previously empty regions depends first on the degree of ionization and, second, on the value of the

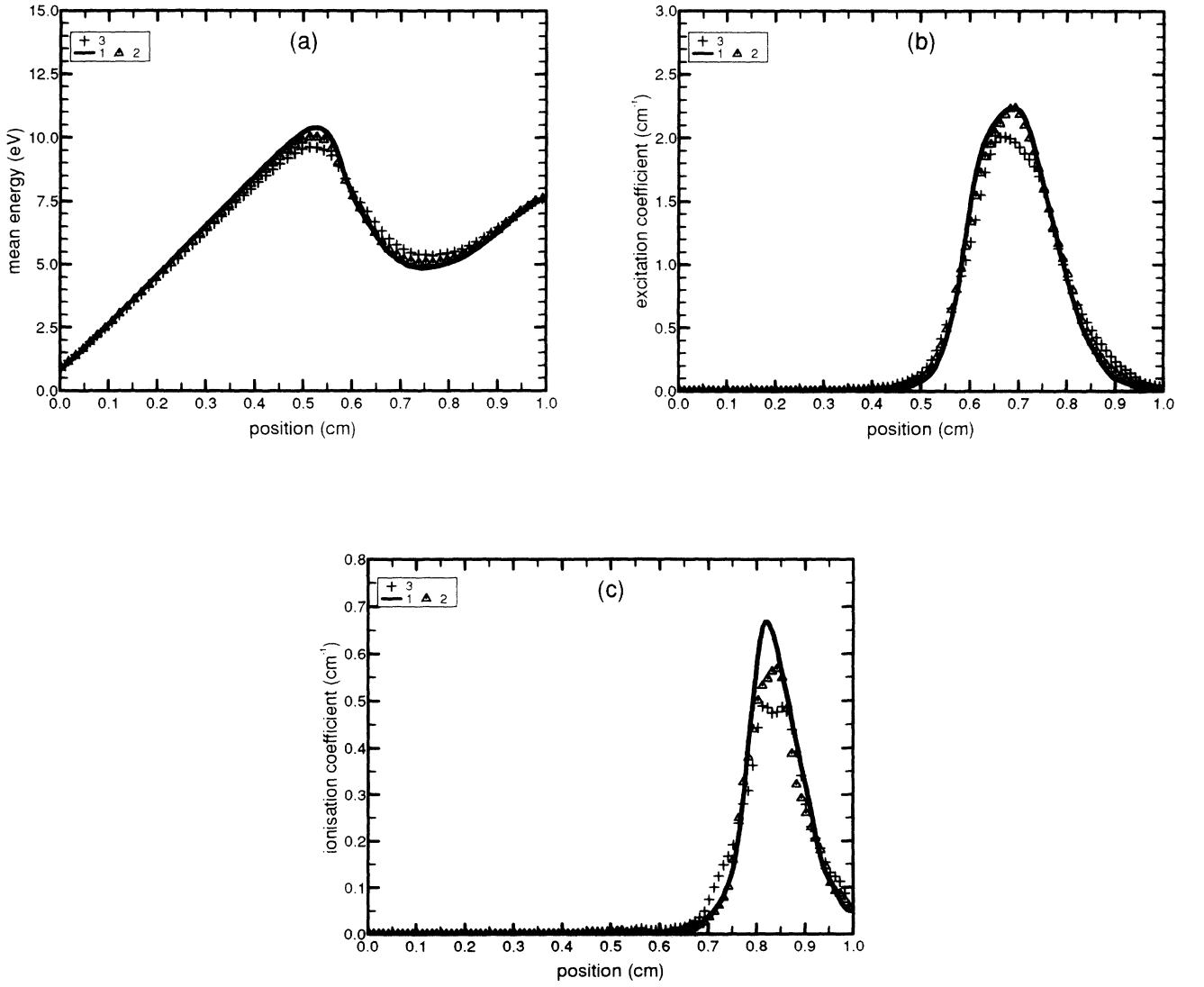

FIG. 7. (a) Space variation of mean energy in argon (1) without electron-electron interactions and with for (2) $n_{e0}/N=10^{-5}$ and (3) $n_{e0}/N=3\times10^{-5}$. The conditions are the same as in Fig. 5. (b) Space variation of excitation coefficients as in (a). (c) Space variation of ionization coefficient as in (a).

electron-electron frequency. It follows that this number of electrons increases when the degree of ionization increases and is greater at low energy as the electron-electron frequency grows [see Figs. 4(b), 4(c), 6(b), and 6(c)].

The effect of electron-electron collisions on the spatial variation of macroscopic parameters can be seen in Figs. 5, 7, and 9. Significant differences appear mainly at low E/N (Figs. 5 and 7). The changes in the mean energy induced by electron-electron interactions are obviously controlled by the spread of electrons in energy space. For example, the decrease and increase in electron mean energy shown in Figs. 5(a) and 7(a) come from the appearance of slow electrons (decrease) and from the appearance of higher energy electrons (increase) between higher and lower energy bands.

The most important effect of electron-electron collisions occurs in the space variation of the excitation and ionization coefficients. In this case, as electrons appear in some regions where there are no electrons if the Coulomb interactions are ignored (where excitation and ionization coefficients are equal to zero), there is a strong increase of

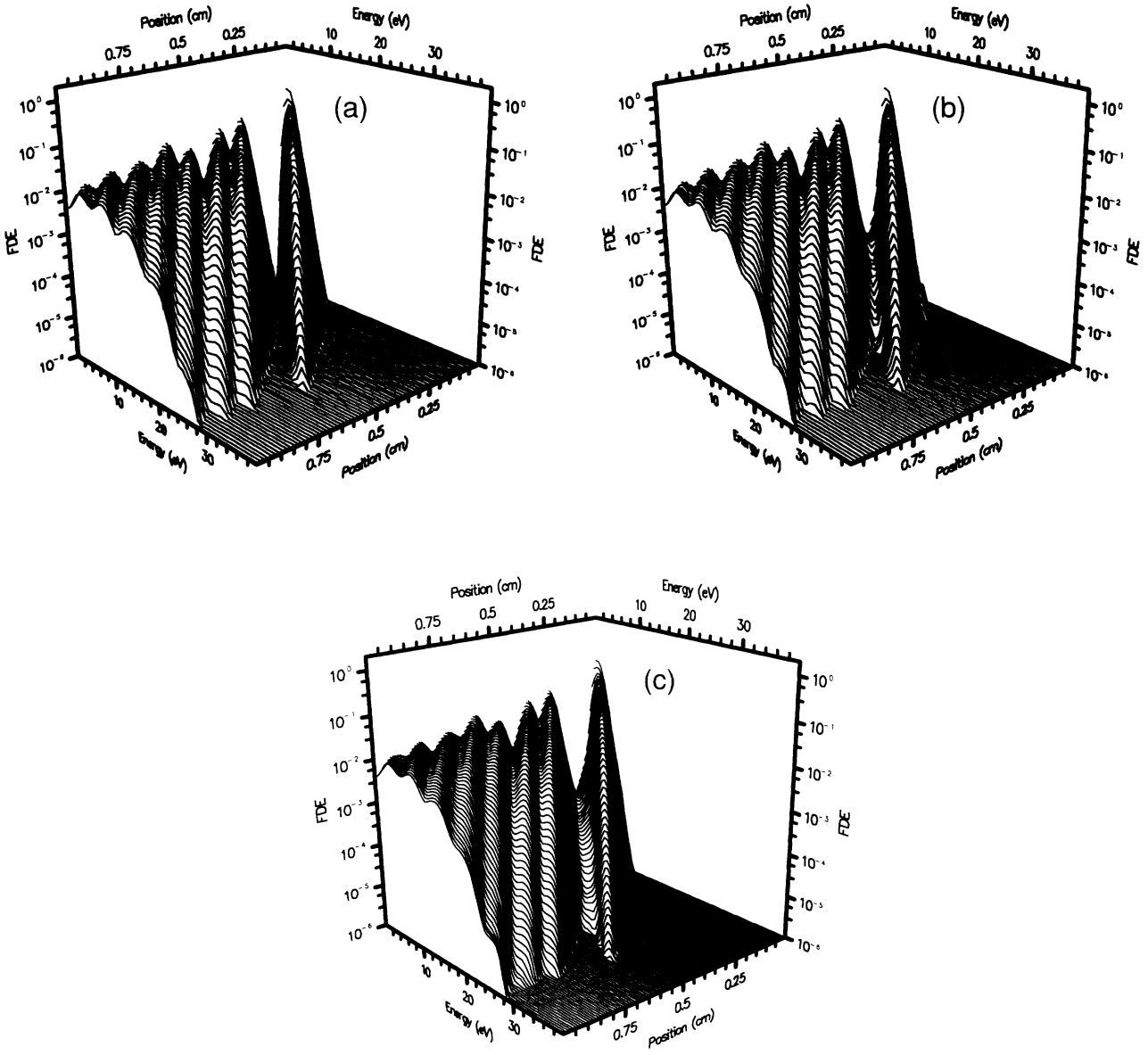

FIG. 8. (a) Energy and space variation of the distribution function in argon without electron-electron interactions for $E/N=141.243$ Td and $Nd=3.54\times10^{+16}$ cm^{-2}. (b) Energy and space variation of the distribution function in argon taking into account the electron-electron interactions for $E/N=141.243$ Td and $Nd=3.54\times10^{+16}$ cm^{-2} $n_{e0}/N=10^{-5}$. (c) Energy and space variation of the distribution function in argon taking into account the electron-electron interactions for $E/N=141.243$ Td and $Nd=3.54\times10^{+16}$ cm^{-2} $n_{e0}/N=3\times10^{-5}$.

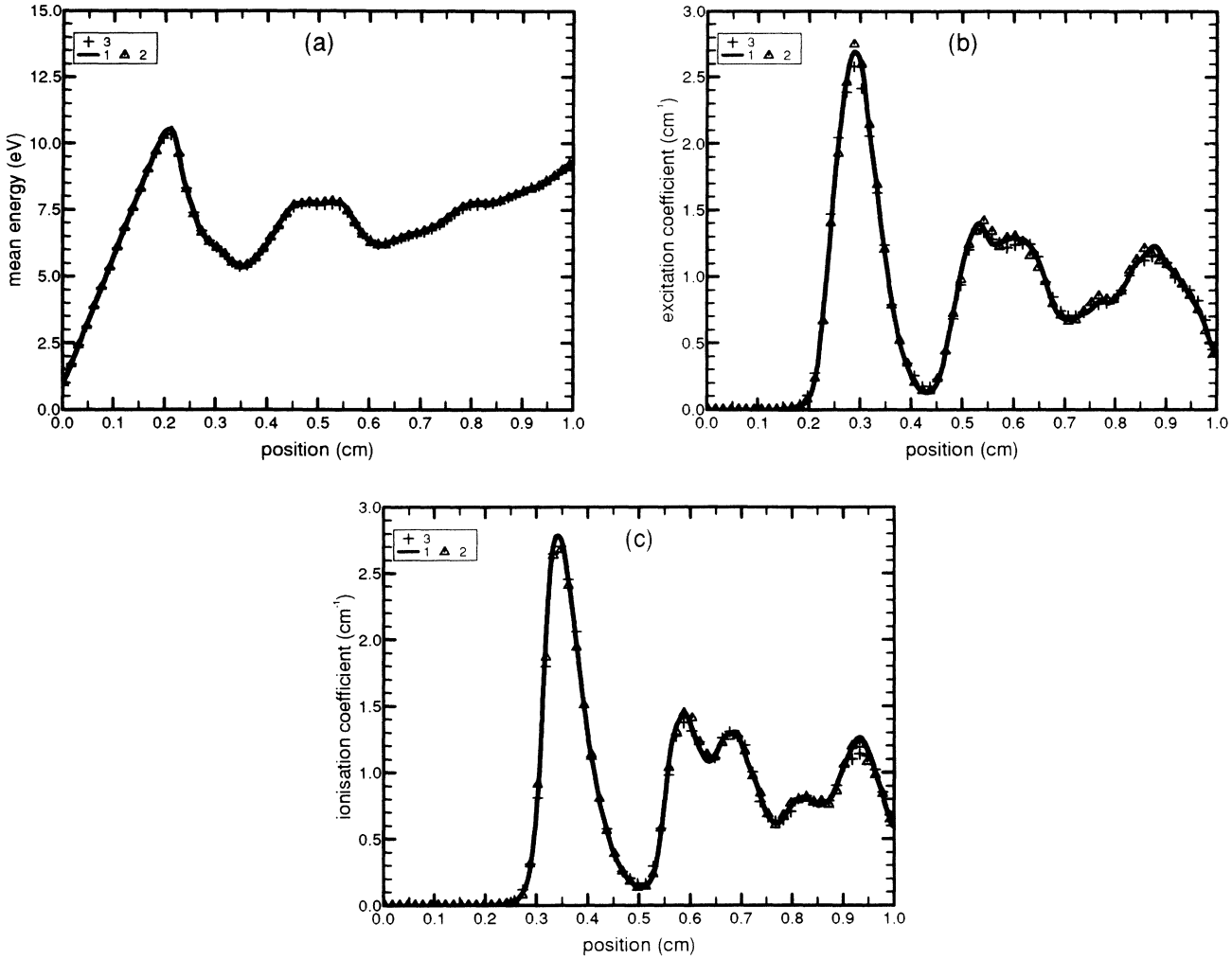

FIG. 9. (a) Space variation of mean energy in argon (1) without electron-electron interactions and with for (2) $n_{e0}/N=10^{-5}$ and (3) $n_{e0}/N=3\times10^{-5}$. The conditions are the same as in Fig. 7. (b) Space variation of excitation coefficient as in (a). (c) Space variation of ionization coefficient as in (a).

excitation and ionization in these regions. On the other hand, there is a strong decrease in regions where the loss of electron energy cannot be balanced by the appearance of electrons coming from higher energies (the first energy band). In the case of Fig. 5(c), near the anode, when the electron-electron interactions are ignored, only a few electrons produce ionization before being absorbed. However, when these interactions are taken into account, more electrons acquire enough energy to produce ionization in the anode region.

It is now clear that the electron-electron interaction effect is more important at low and intermediate E/N values than at high E/N. In this case, as the various bands overlap [Figs. 8(a) and 8(b)], electrons coming from electron-electron interactions do not play a large role. Furthermore, the electron mean energy being higher, the electron-electron frequency is lower. It is then not surprising that the space variation of the various macroscopic parameters is the same as in the case where electron-electron interactions are ignored (Fig. 9).

Regarding these results overall, we can say that the global effect of the electron-electron interactions is to balance the energy between the electrons, allowing them to move in a large phase space, making the energy distribution function tend toward a Maxwellian distribution and the swarm parameters get closer to their equilibrium values.

V. CONCLUSION

In this paper we developed a method to include in a rigorous way electron-electron interactions in a Monte Carlo treatment. Unlike in some previous studies, the treatment was made rigorous by taking full account of the kinetics of electron-electron collisions in the Monte Carlo process. This method was checked in some simple situations and was shown to be able to predict basic physical properties. A study was made of the transport of electrons in a simple gaseous discharge and the importance of electron-electron interactions was shown for different degrees of ionization and different E/N values. Our future work will be devoted to the study of the importance of electron-electron collisions in the transition between the cathode fall and the negative glow of an abnormal glow discharge.

[1] H. Dreicer, Phys. Rev. **117**, 343 (1960).
[2] B. E. Cherrington, *Gaseous Electronics and Gas Lasers* (Pergamon, New York, 1979).
[3] A. Gillardini, *Low Energy Electron Collisions in Gases* (Wiley, New York, 1972).
[4] J. A. Bittencourt, *Fundamentals of Plasma Physics* (Pergamon, New York, 1990).
[5] S. D. Rockwood, J. Appl. Phys. **45**, 5229 (1974).
[6] M. Yousfi, G. Zissis, A. Alkaa, and J. J. Damelincourt, Phys. Rev. A **42**, 978 (1990).
[7] A. Alkaa, doctorat de l'Université Paul Sabatier, No. 967, Université Paul Sabatier, 1991.
[8] P. K. Milsom, J. Phys. D **25**, 1086 (1992).
[9] J. P. Boeuf and E. Marode, J. Phys. D. **15**, 2069 (1982).
[10] I. D. Reid, Aust. J. Phys. **32**, 231 (1979).
[11] B. M. Penetrante, J. N. Bardsley, and L. C. Pitchford, J. Phys. D. **18**, 1087 (1985).
[12] J. P. Boeuf, thèse de doctorat d'état, No. 3043, Université de Paris Sud, Orsay, 1985.
[13] M. Terissol, thèse de doctorat ès-sciences, No. 839, Université Paul Sabatier, Toulouse, 1978.
[14] H. R. Skullerud, J. Phys. D **1**, 1567 (1968).
[15] S. L. Lin and J. N. Bardsley, J. Chem. Phys. **66**, 435 (1977).
[16] S. L. Lin and J. N. Bardsley, Comput. Phys. Commun. **15**, 161 (1978).
[17] A. Chouki (personal communication).

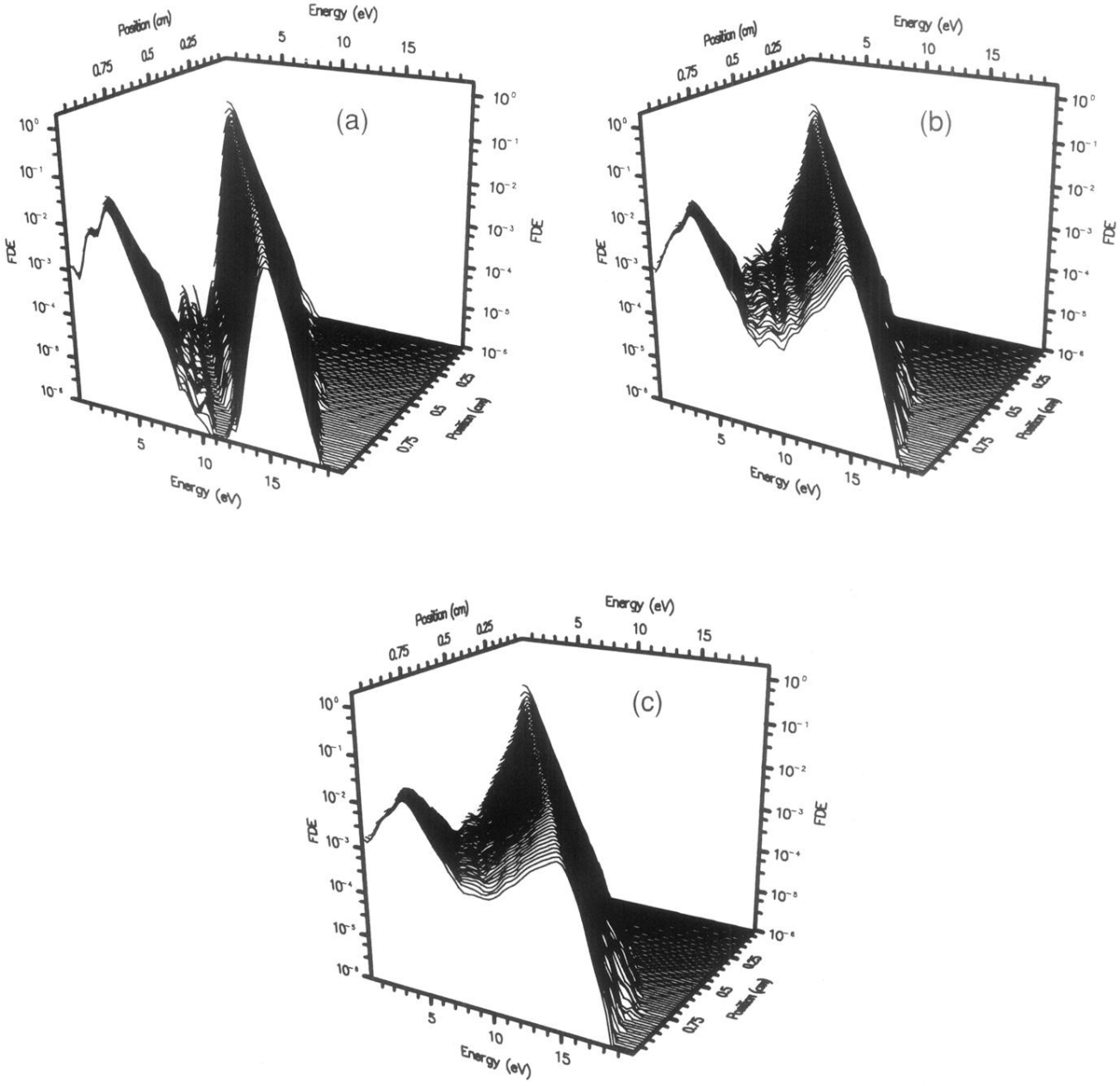

FIG. 4. (a) Energy and space variation of the distribution function in argon without electron-electron interactions for $E/N=42.373$ Td and $Nd=3.54\times10^{+16}$ cm^{-2}. (b) Energy and space variation of the distribution function in argon taking into account the electron-electron interactions for $E/N=42.373$ Td and $Nd=3.54\times10^{+16}$ cm^{-2} $n_{e0}/N=10^{-5}$. (c) Energy and space variation of the distribution function in argon taking into account the electron-electron interactions for $E/N=42.373$ Td and $Nd=3.54\times10^{+16}$ cm^{-2} $n_{e0}/N=3\times10^{-5}$.

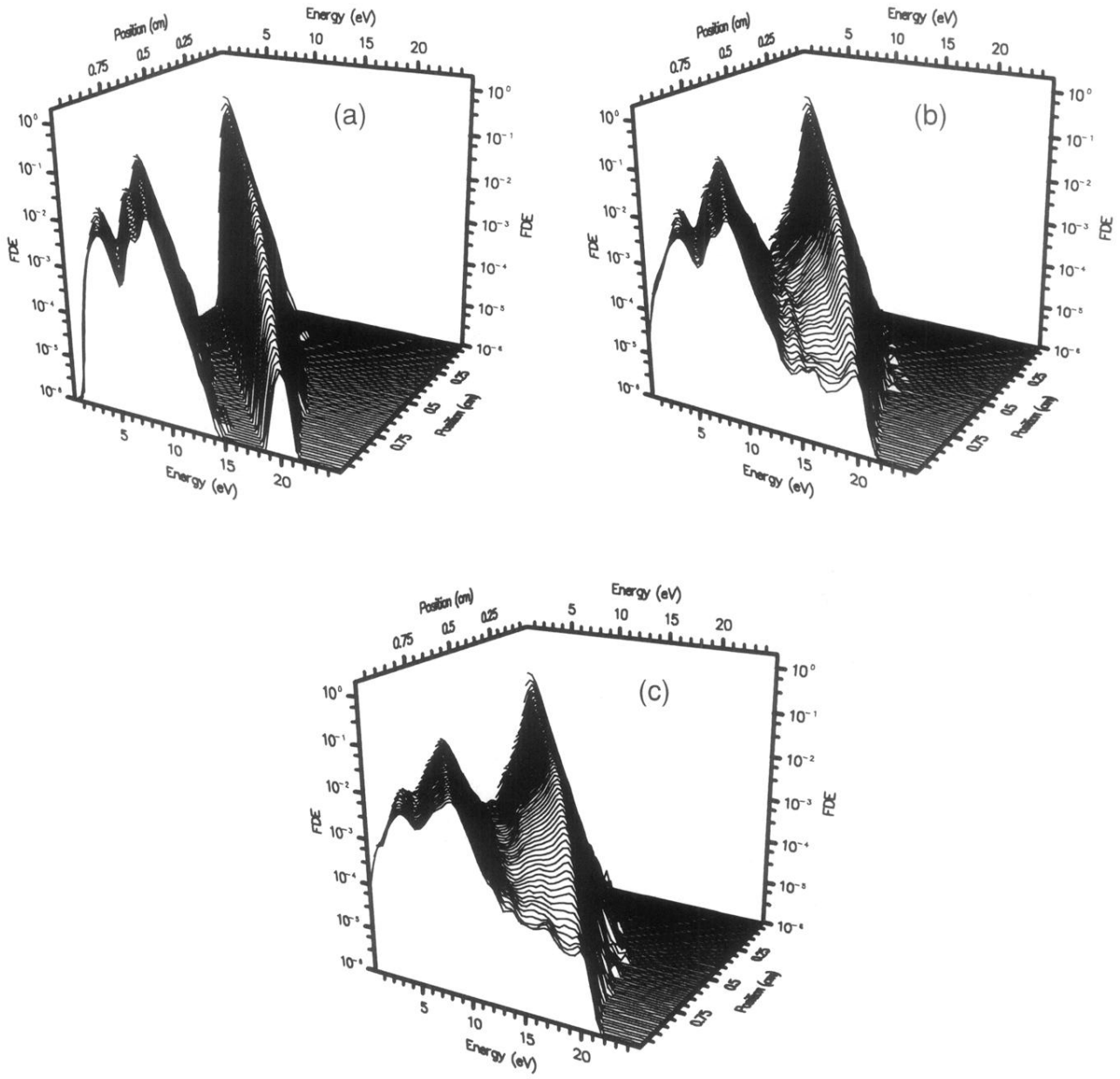

FIG. 6. (a) Energy and space variation of the distribution function in argon without electron-electron interactions for $E/N=56.497$ Td and $Nd=3.54\times10^{+16}$ cm^{-2}. (b) Energy and space variation of the distribution function in argon taking into account the electron-electron interactions for $E/N=56.497$ Td and $Nd=3.54\times10^{+16}$ cm^{-2} $n_{e0}/N=10^{-5}$. (c) Energy and space variation of the distribution function in argon taking into account the electron-electron interactions for $E/N=56.497$ Td and $Nd=3.54\times10^{+16}$ cm^{-2} $n_{e0}/N=3\times10^{-5}$.

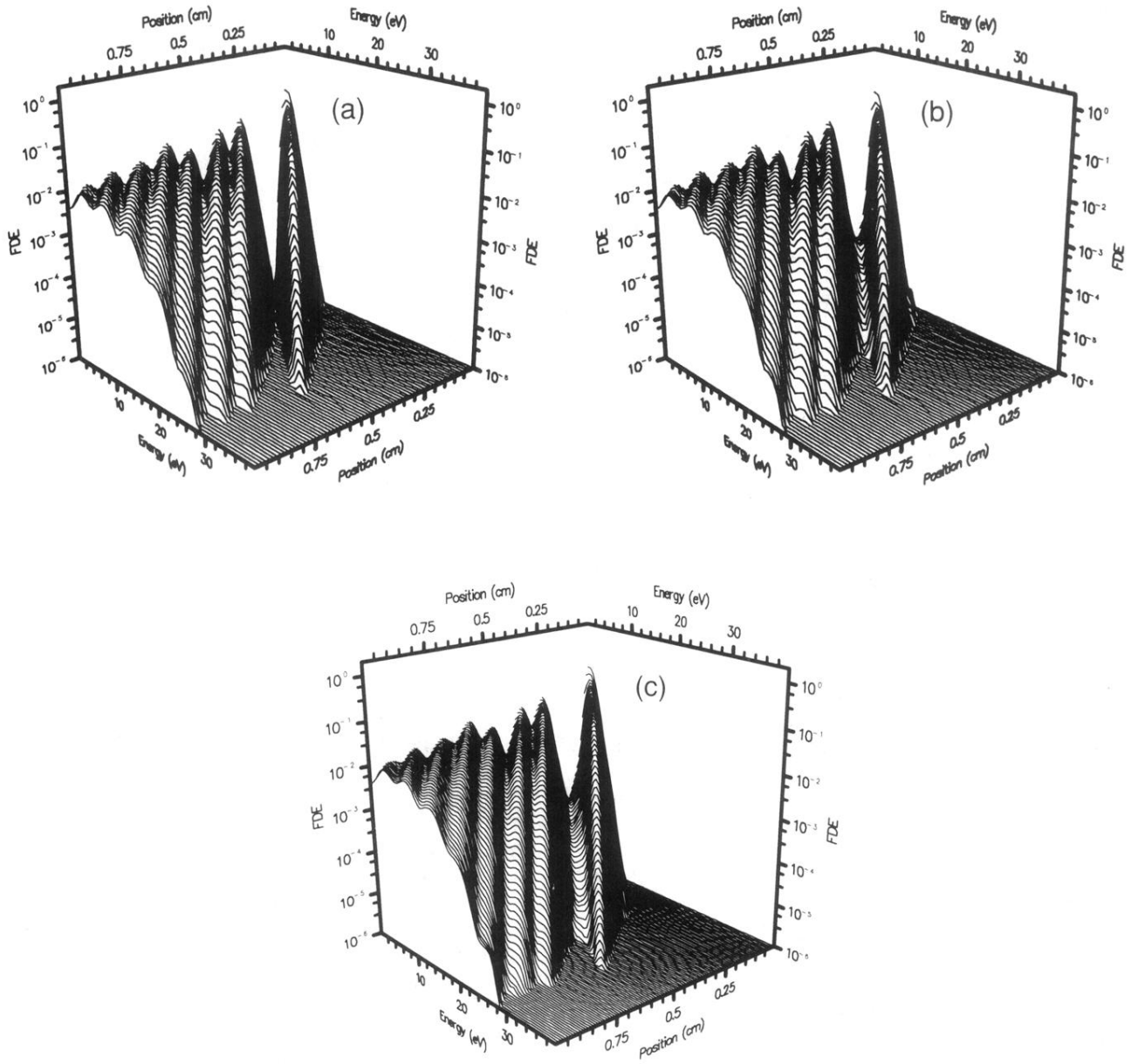

FIG. 8. (a) Energy and space variation of the distribution function in argon without electron-electron interactions for $E/N=141.243$ Td and $Nd=3.54\times10^{+16}$ cm^{-2}. (b) Energy and space variation of the distribution function in argon taking into account the electron-electron interactions for $E/N=141.243$ Td and $Nd=3.54\times10^{+16}$ cm^{-2} $n_{e0}/N=10^{-5}$. (c) Energy and space variation of the distribution function in argon taking into account the electron-electron interactions for $E/N=141.243$ Td and $Nd=3.54\times10^{+16}$ cm^{-2} $n_{e0}/N=3\times10^{-5}$.